Numerical tensile test on a mushy zone sample

Jean-François Zaragoci, Luisa Silva, Michel Bellet, Charles-André Gandin

Proc. MCWASP XIII, 13th Int. Conf. on Modelling of Casting, Welding and Advanced Solidification Processes, Schladming (Austria), June 17-22, 2012, A. Ludwig, M. Wu, A. Kharicha (eds.), IOP Conference Series 33 (2012) 012054

Numerical tensile test on a mushy zone sample

Jean-François Zaragoci, Luisa Silva, Michel Bellet, Charles-André Gandin
MINES ParisTech CEMEF, UMR CNRS 7635, 06904 Sophia Antipolis, France

E-mail: luisa.silva@mines-paristech.fr

Abstract. Time sequences of 3D images of an Al-Cu alloy in the mushy state are obtained using in situ and real-time X-ray microtomography during a tensile test. Surface meshes of phase interfaces are built from these images with the help of a Marching Cubes algorithm. The signed distance to the surface meshes is then computed on a finite element mesh of the volume of the phases. These signed distance functions enable to track the interfaces between the phases in an implicit way. A numerical representation of the real microstructure is thus obtained, allowing to perform a numerical tensile test which is compared with the experimental tensile test. Results retrieve the general dynamic behaviour of the strain field evolution and opens promising perspectives for further interpretations of experimental results based on numerical simulations.

1. Introduction

Nowadays, numerical simulations of complex systems are mandatory in many fields. The first aspect to consider for performing analyses on such system is the creation of a realistic numerical representation of the object under study. This is the case in phase transformations taking place in the context of materials science. Several phases may coexist in a given material, delimited by interfaces. A mesh of the structure of the phases is then needed to study the heat, mass and momentum transfers taking place at phase interfaces and in the bulk phases. Results of such analyses for the entire material are not trivial because of the various phase properties and interface behaviours.

When it is not possible to consider a numerical representation of the real specimen, statistical representative elementary volumes (REV) can be used. Advantages lead in the possibility to easily change the morphology of the REV. The sample behaviour can then be studied with respect to various parameters. For instance, by using a modified Voronoi tessellation, Phillion et al. showed the effect of microstructural features on the semi-solid tensile deformation of an aluminium alloy such as solid fraction, porosity and grain size [1].

During the last decade, X-ray microtomography has considerably developed [2-4]. This imaging technique gives access to in situ three-dimensional (3D) morphology of a multiphase sample. Thus, Terzi et al. obtained a set of 3D images showing morphological evolutions in a few millimeters sample of an aluminium copper alloy during tensile testing [5]. It is currently possible to reach a spatial and time resolution of less than 1 µm and 1 s, respectively, on millimeters domain size [4].

The ambition of this paper is to describe a way to transform data coming from X-ray microtomography into a finite element (FE) representation and to use it to run numerical simulations. In section 2, the approach chosen to obtain the FE representation is explained. Section 3 presents the model equations for the numerical tensile test and the way to solve them. Finally, results on the real morphology are presented and compared to the experimental data in section 4.

2. Finite element representation

Three steps are required to transform a 3D picture into a FE representation [6]: segmentation, surface mesh computation and volume mesh computation. The segmentation is the designation of all the phases of the multiphase domain, using the grey level of the tomography images. Because images are already segmented by Terzi et al. [5], only generations of surface and volume mesh will be explained here.

1.0. Surface mesh computation

The surface meshes used to separate the different phases are a representation of the interfaces between these phases. In the case considered here, three phases are identified with the X-ray microtomography: solid, liquid and air. Two segmentations give access to two binary images, where only black and white levels are present to separate the liquid phase from the solid+gas zone and the gas from the solid+liquid zone. These two images are sufficient to define all solid/liquid, solid/gas and liquid/gas interfaces. Two surface meshes are then computed with the help of a Marching Cubes (MC) algorithm. Voxels are the constitutive element of 3D images. A 3D image can be seen as a stack of 2D slices. A marching cube is a logical cube created from eight neighbouring voxels, four from one slice and four from the neighbouring slice [7]. For each voxel, two states are possible: inside a phase or outside it. Consequently there are $2^8 = 256$ cases for a MC. Each case corresponds to a surface separating the phases. To obtain the surface, rotational symmetry is considered [8] to reduce the problem from 256 cases to 23 patterns shown in figure 1. Once the surface is computed for one MC, the algorithm moves to the next cube until the whole image is treated.

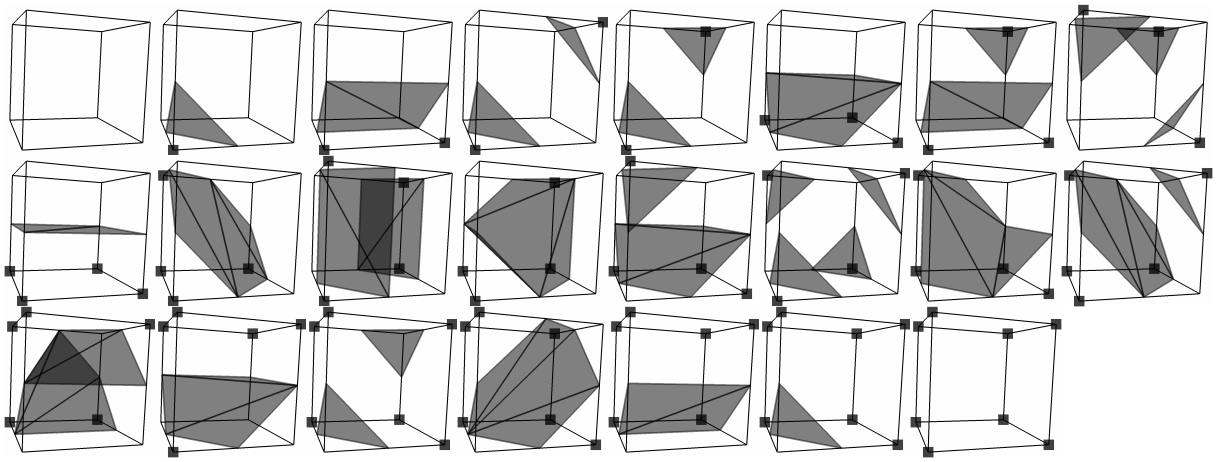

Figure 1. Illustration of the 23 patterns considered for a single marching cube and corresponding surface mesh. Vertices are assigned a dot if they are inside the liquid.

1.0. Volume mesh computation

The volume mesh computation is based on the immersed volume method (IVM) described in [9]. In our case the volume mesh used for tensile test computations must include, as for the images, three existing phases. Two level set functions are computed within this volume mesh to take into account the properties of the three phases.

A level set function is a signed distance from a surface mesh computed for all nodes of our tetrahedral volume mesh. Two level sets are computed: the liquid level set ϕ_l, representing the interface between the liquid and the solid+gas mixture, and the air level set ϕ_a, representing the interface between the air and the solid+liquid mixture. The negative sign for the liquid level set is chosen inside the liquid and inside the air for the air level set. The algorithm used to compute the distance between a triangular facet of the surface mesh and a node of the volume mesh is described

in [11]. To get the signed distance, the normal to the facet of the surface mesh is used. The distance between a node and the surface mesh is the minimal distance between this node and all the facets. Because surface and volume meshes can have several millions of facets and nodes respectively, it is very time consuming to compute the distance from a given node to all the facets of the surface mesh. To decrease the CPU time cost, a hierarchical representation of the surface mesh is built at the beginning of the simulation [12].

With the IVM, each equation treated is solved on the whole computational domain [9]. Behaviour of all phases vary from Newtonian to viscoplastic, meaning that all the physical properties necessary for a simulation are defined in the whole volume mesh using a classical mixture law of the properties of each phase and the level sets defining the interfaces. In the immediate neighbourhood of an interface separating two phases, 1 and 2, a piecewise continuous mixing model is used. A mixed property α is thus defined as:

$$\alpha = H\alpha_1 + (1-H)\alpha_2 \tag{1}$$

α_1 and α_2 are the property values for the two phases considered and H is the filling ratio of the element for phase 1, computed with the level set separating the two phases. With three phases, equation (1) is applied twice to take into account the two level sets and the properties of all the phases. In a first time, the air level set is used with air and liquid properties. Then, the solid level set, viz. the opposite of the minimum of air and liquid level sets, is used with solid properties and the results of the first mixture.

A topological mesher [10] is used with only isotropic meshes in this paper.

1. Numerical model

2.1. Equations

Simulating the morphological evolutions of a sample at this scale is a highly challenging multiphysics problem. In this work, the physical models chosen to simulate the tensile test of the aluminium copper alloy are simplified.

1.0.0. Mechanical behaviour. Because inertial and mass terms are assumed negligible, only the Stokes equations without right hand member are solved:

$$\nabla \cdot \bar{\bar{\sigma}} = \vec{0} \tag{2}$$

$$\nabla \cdot \vec{v} = 0 \tag{3}$$

$\bar{\bar{\sigma}}$ is the stress tensor and $\vec{v}$ the velocity vector of the flow. The liquid and the air are modelled as two incompressible Newtonian fluids. The stress tensor inside these phases reads:

$$\bar{\bar{\sigma}} = 2\eta\bar{\bar{\varepsilon}}(\vec{v}) - p\bar{\bar{I}} \tag{4}$$

η is the viscosity, $\bar{\bar{\varepsilon}}(\vec{v})$ the strain rate tensor and $\bar{\bar{I}}$ the identity tensor. For the solid phase, neglecting elasticity, the behaviour is viscoplastic. Stress and strain rate are related by:

$$\bar{\bar{\sigma}} = 2\eta_{eq}\bar{\bar{\varepsilon}}(\vec{v}) - p\bar{\bar{I}} = 2\left(\frac{K}{3}\dot{\varepsilon}^{m-1}\right)\bar{\bar{\varepsilon}}(\vec{v}) - p\bar{\bar{I}} \tag{5}$$

K is the consistency, m the strain rate sensitivity, $\dot{\bar{\varepsilon}}$ the equivalent strain rate and η_{eq} the apparent solid viscosity. The corresponding relation between the equivalent stress $\bar{\sigma}$ and $\dot{\bar{\varepsilon}}$ is:

$$\bar{\sigma} = K\dot{\bar{\varepsilon}}^{m} \tag{6}$$

1.0.0. Interfaces displacements. To keep the interfaces still represented by the zero isovalue of the level set functions while updating the configuration, the level sets should be moved with the velocity derived from the resolution of the Stokes equations. To this purpose, the following convection equation is solved for ϕ_l and ϕ_a :

$$\frac{\partial \phi}{\partial t} + \vec{v} \cdot \vec{\nabla}\phi = 0 \tag{7}$$

After solving equation (7), the level set functions are no longer signed distance functions. To recover this property at times t when judged necessary, a reinitialisation equation is solved [13]:

$$\frac{\partial \phi}{\partial \tau} = S(\phi)\left(1 - \left\|\vec{\nabla}\phi\right\|\right) \tag{8}$$

$S(\phi)$ is the sign of the level set whereas τ is a fictitious time step linked to the mesh size. To speed up the computation, equation (7) and equation (8) are coupled to obtain a convective reinitialisation equation [14]. Moreover, the level set functions being useful only near the interfaces, a smoothed function is rather used, through the hyperbolic tangent of the distance to each interface [15].

1.0. Finite elements

The partial derivative equations are solved with the finite element method with CIMLib, a highly parallel C++ scientific computation library described in [16], using PETSc [17] (Portable, Extensible Toolkit for Scientific Computation) for solving the linear systems and MPI (Message Passing Interface) for the parallelism.

1.0.0. Stokes equations. After mixing the consistency and the strain rate sensitivity of the three phases, Stokes equations are solved with the method introduced in [18], known as MINI-element, which satisfies the Brezzi-Babuška stability condition [19]. The linear system is solved with the conjugate residual method associated with an incomplete LU preconditioning [20]. To consider the non linear behaviour of the solid phase, the fixed point method is used: once the velocity field $\vec{v}$ is computed, a new equivalent strain rate $\dot{\bar{\varepsilon}}$ is obtained, giving rise to a new estimate for the viscosity η_{eq} to be considered for the next resolution of equation (2).

2.1.1. Convective reinitialisation equation. The standard Galerkin method leading to results with spurious oscillations well known for hyperbolic problems, a streamline upwind Petrov-Galerkin (SUPG) stabilisation method is employed [21]. The linear system is solved with the generalized minimal residual method (GMRES) [22] and an incomplete LU preconditioning.

3. Results

3.1. Finite element representation

Given its morphological complexity [5], accurate representation of the sample implies a very large number of nodes, leading to long and difficult subsequent simulations. Thus, an isotropic mesh size of 10 µm is used whereas the initial voxel size is 2.8 µm. Moreover, only a quarter of the sample is modelled. Despite these considerations, the volume mesh contains more than 3 million nodes and 16 million elements. Figure 2a shows the experimental interface between the air and the liquid+solid mixture 513 s after the beginning of the tensile test. It is attained from microtomography data with voxel representation. Figure 2b shows the same interface drawn for the FE numerical representation. The CPU time for computing the surface mesh is 14 s with one processor (RAM: 3.25 Go, 2.99 GHz Intel Core CPU). The CPU time for computing the air level set is less than 5 min with 16 processors (2.4 GHz Opteron cores linked by an Infiniband network). Excellent geometrical reconstruction of the domain boundaries with the FE mesh is demonstrated, only limited by the size of the FE mesh used.

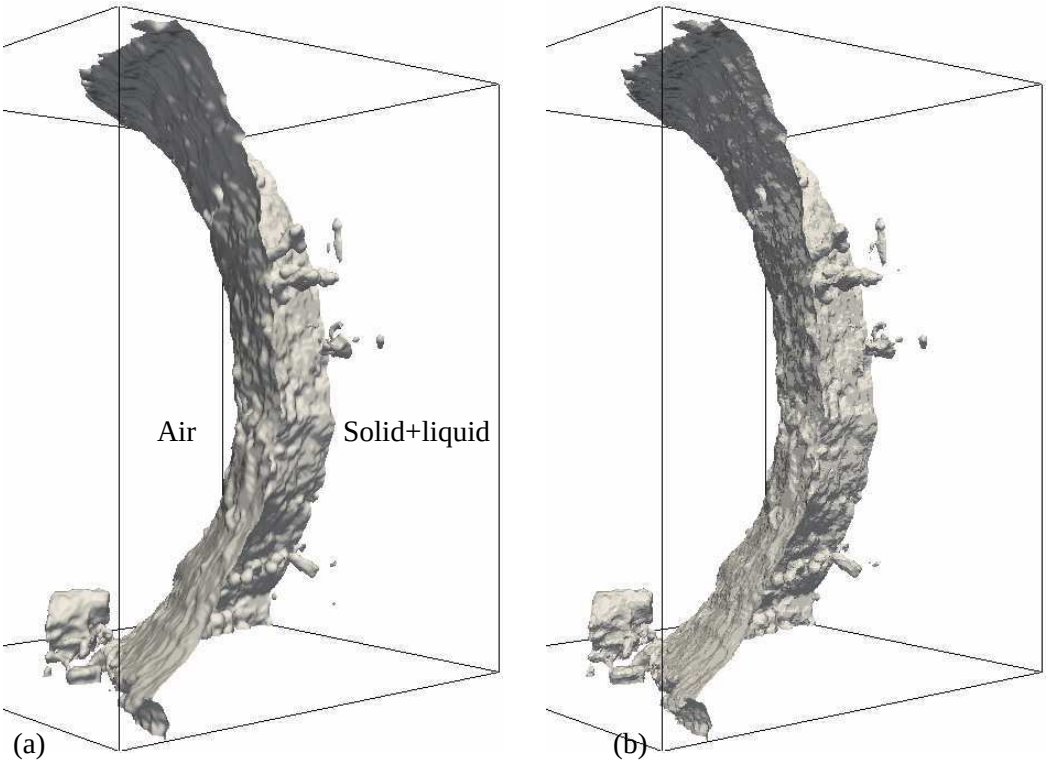

Figure 2. Metallic sample boundary between the air and the solid+liquid mixture 513 s after the beginning of the tensile test. (a) Experimental and (b) numerical boundaries. Vertical field of view: 1.43 mm.

1.0. Mechanical computation

Boundary conditions are applied for a uniaxial vertical tensile test. A vertical velocity is imposed at the bottom and at the top of the sample on all phases and vertical symmetry conditions are applied. To match the experimental conditions, the velocity at the bottom is zero and the velocity at the top is 0.1 $\mu m.s^{-1}$. For the solid, parameters are taken from a compression test campaign similar to the one made by [23], leading to m = 0.2 and K = 35.2 MPa. The apparent solid viscosity is on the order of 10^{10} Pa.s whereas viscosities to be considered are about 10^{-5} Pa.s for the air and 10^{-3} Pa.s for the liquid. With these values, the ratio between minimal and maximal viscosities is very large and no solution is found

for the Stokes equations, due to a very bad conditioning of the global matrix and a limited precision. It is thus necessary to use augmented viscosities. For the liquid and the air, viscosities used in the simulations are 100 kPa.s and 1 kPa.s, respectively. These values are large by comparison with real values, but the ratio with the apparent solid viscosity is still significant and stress inside the air and the liquid are negligible. Figure 3 shows the equivalent strain rate and the equivalent stress of a 2D cross sectional cut 513 s after the beginning of the tensile test, assuming a static mechanical state. It can be seen that maximum strain rate values are found in liquid pockets. Stresses are quite heterogeneous in the solid, showing maximum values in specific regions, especially between liquid regions.

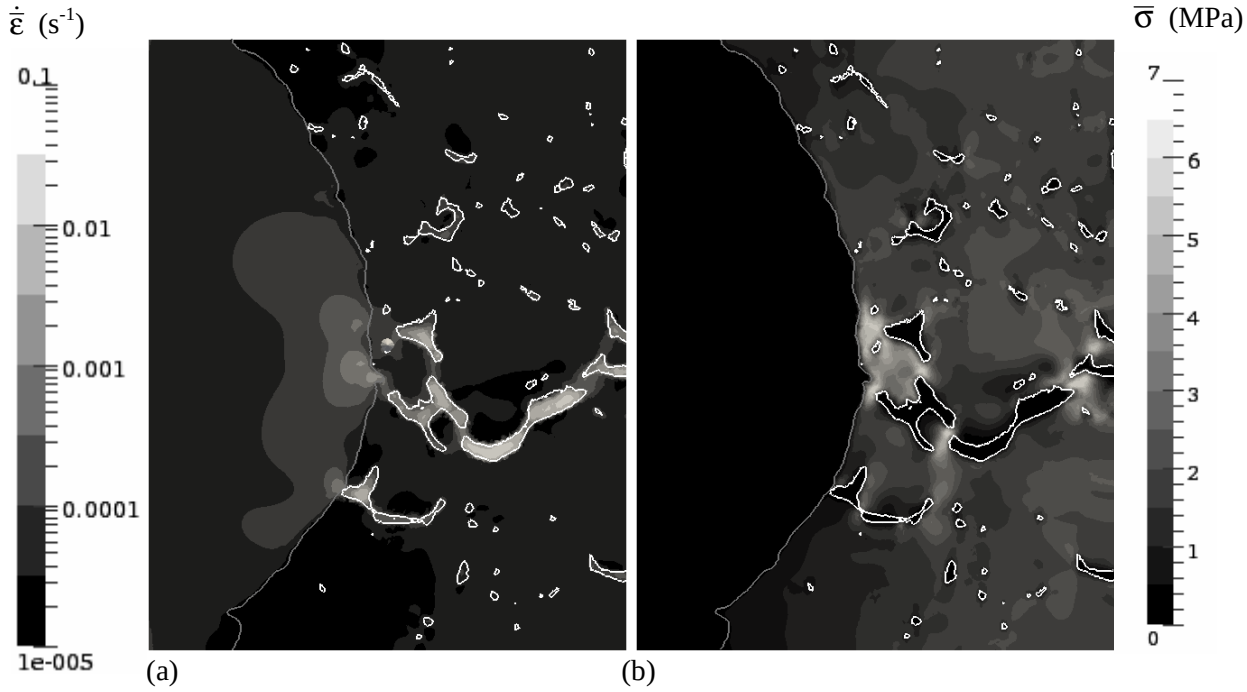

Figure 3. Mechanical results for a 2D cross sectional cut of figure 2b. (a) Equivalent strain rate and (b) equivalent stress. Grey and white contours represent the zero isovalue of the air and liquid level sets respectively, i. e. boundaries between phases.

3.2. Dynamic computation

For the experiment described in [5], a lot of X-ray images are available at incremental times. It then becomes possible to compute the associated numerical representations to perform static mechanical computations, i. e. without moving the interfaces, as in the previous section. This leads to as many calculations as recorded images with time. But the model is also developed to start with one numerical representation taken as initial condition, then solve the Stokes equations, move the interfaces and continue in a time stepping loop, until the end of the experiment. Thanks to this dynamic simulation, comparisons can be made between the evolution of experimental and numerical morphologies of the interfaces. Figure 4 illustrates such a comparison for the interface between the air and the liquid+solid mixture 1323 s after the beginning of the tensile test. To obtain this reasonable agreement with the observation using X-ray microtomography, the starting numerical representation is the one shown in figure 2, just before experimental penetration of air in the sample. The CPU time for computing this evolution is four days with 50 processors (2.4 GHz Opteron cores linked by an Infiniband network) and a time step of 13.5 s. To corroborate this qualitative comparison, the equivalent stress evolution in the solid phase is compared for the static and the dynamic computations in figure 5. Both curves show a stress decrease due to sample damage by air propagation.

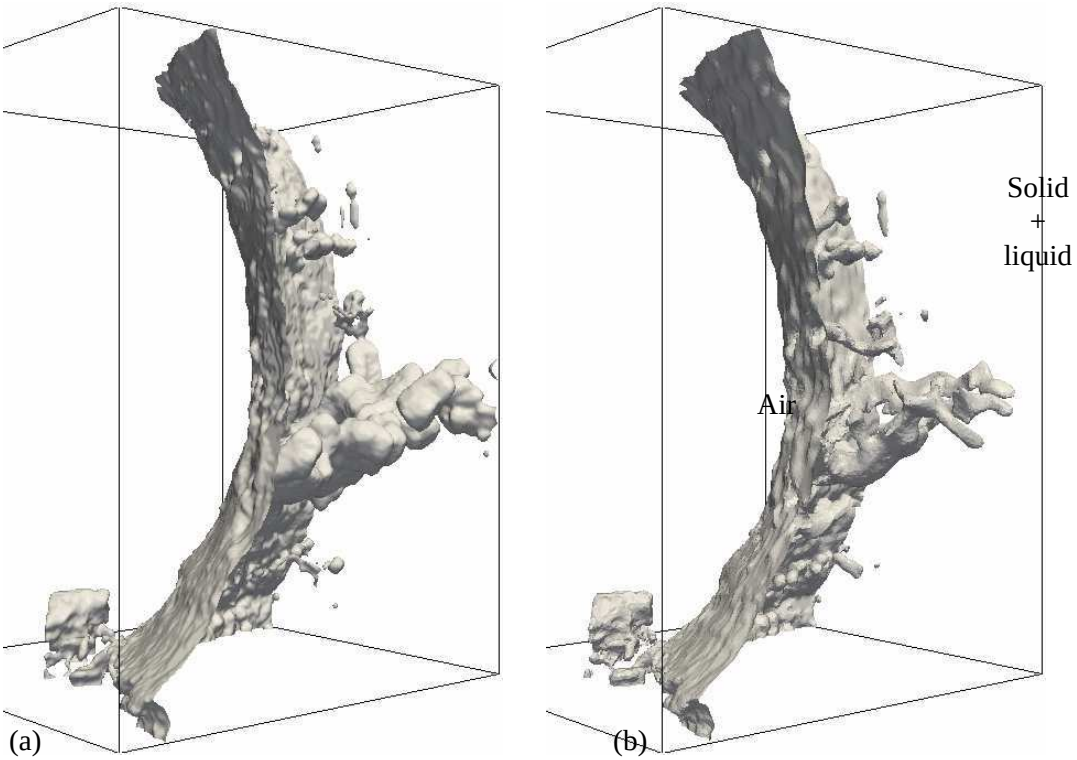

Figure 4. Boundary between the air and the solid+liquid mixture 1323 s after the beginning of the tensile test. (a) Experimental and (b) numerical boundaries. Vertical field of view: 1.43 mm.

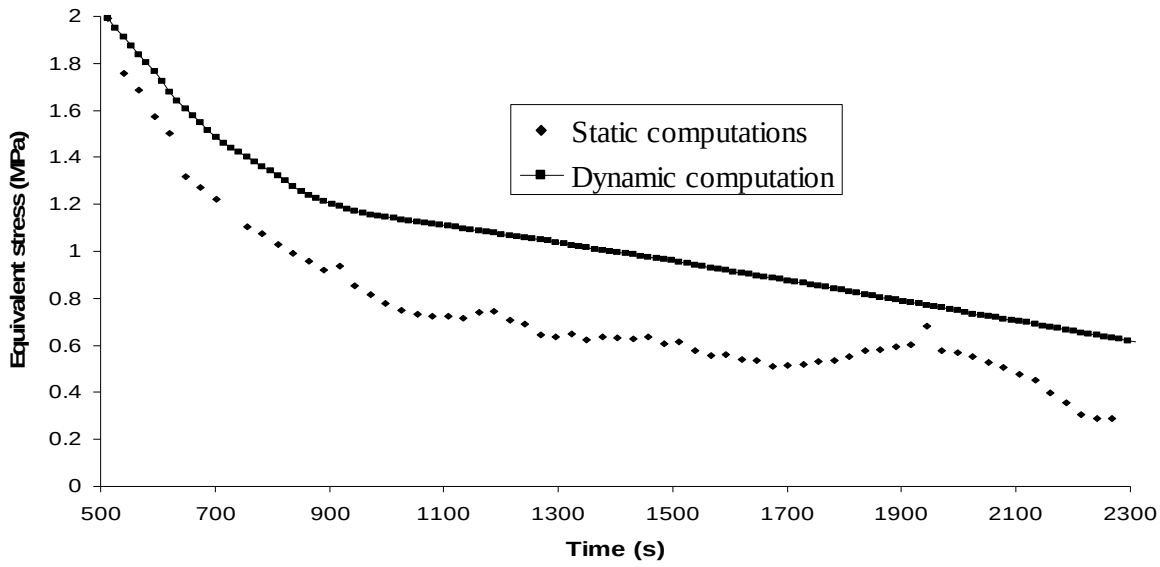

Figure 5. Equivalent stress evolution in the solid phase for static and dynamic computations.

4. Conclusion & perspectives

Transformation of X-ray microtomography data into tetrahedral 3D finite element representations has been presented in this paper, using implicit interface description with the help of level set functions. By solving conservation equations with initial and boundary conditions similar with experiments,

direct comparisons between numerical and experimental results are possible. Comparisons made for a tensile test on a mushy zone sample are realistic and motivate further work.

Perspectives include: (i) more complex models taking into account solidification and additional physical phenomena such as surface tension, wetting and gas solubility, (ii) better interface representation with anisotropic meshes, (iii) larger computation to simulate the entire sample and increase space resolution. Such efforts could be conducted in parallel to more accurate experiments to gain advantage of microtomography recent progresses and development of image correlation tools to better estimate the boundary conditions to apply from experimental data.

Acknowledgements
This work was carried out in the framework of the project ANR-08-BLANC-0062 “SIMUZAL”, supported by the “Agence Nationale de la Recherche”, which is gratefully acknowledged. The authors would especially like to thank Bastien Mireux, Michel Suéry and Luc Salvo for providing them the experimental images and the results of the compression test campaign used in this work.

References

[1] Phillion A B, Cockcroft S L and Lee P D 2008 *Acta Mater.* **56** 4328
[2] Salvo L, Cloetens P, Maire E, Zabler S, Blandin J J, Buffière J-Y, Ludwig W, Boller E, Bellet D and Josserond C 2003 *Nucl. Instrum. Meth. B* **200** 273
[3] Baruchel J, Buffière J-Y, Cloetens P, Di Michiel M, Ferrie E, Ludwig W, Maire E and Salvo L 2006 *Scripta Mater.* **55** 41
[4] Salvo L, Suéry M, Marmottant A, Limodin N and Bernard D 2010 *C. R. Phys.* **11** 641
[5] Terzi S, Salvo L, Suéry M, Limodin N, Adrien J, Maire E, Pannier Y, Bornert M, Bernard D, Felberbaum M, Rappaz M and Boller E 2009 *Scripta Mater.* **9** 449
[6] Madi K, Forest S, Boussuge M, Gailliègue S, Lataste E, Buffière J-Y, Bernard D and Jeulin D 2007 *Comp. Mater. Sci.* **39** 224
[7] Lorensen W-E and Cline H-E 1987 *Comput. Graphics* **21** 163
[8] Nielson G M, Huang A and Sylvester S 2002 *IEEE Visualization* (Boston) 459
[9] Hachem E, Kloczko T, Digonnet H and Coupez T 2010 Stabilized finite element solution to handle complex heat and fluid flows in industrial furnace using the immersed volume method *Int. J. Numer. Meth. Fl.* online http://dx.doi.org/10.1002/fld.2498
[10] Gruau C and Coupez T 2005 *Comput. Method. Appl. M.* **157** 115
[11] Schneider P and Eberly D 2002 *Geometric Tools for Computer Graphics* (Elsevier Science Inc., New York)
[12] Bruchon J, Digonnet H and Coupez T 2009 *Int. J. Numer. Meth. Eng.* **78** 980
[13] Sussman M, Smereka P and Osher S 1994 *J. Comput. Phys.* **114** 146
[14] Ville L, Silva L and Coupez T 2011 *Int. J. Numer. Meth. Fl.* **66** 324
[15] Coupez T 2011 *J. Comput. Phys.* **230** 2391
[16] Digonnet H, Silva L and Coupez T 2007 *Proc. NUMIFORM* (Porto) **208** 269
[17] Balay S, Buschelman K, Eijkhout V, Gropp W, Kaushik D, Knepley M, Curfman McInnes L, Smith B and Zhang H *PETSc Users Manual – Revision 3* (Mathematics and Computer Science Division, Argonne National Laboratory)
[18] Arnold D, Brezzi F and Fortin M 1984 *Calcolo* **23** (4) 337
[19] Babuška I 1973 *Math. Comput.* **27** (122) 221
[20] Saad Y 2003 *Iterative Methods for Sparse Linear Systems* (SIAM)
[21] Brooks A N and Hughes T J R 1982 *Comput. Method. Appl. M.* **32** 199
[22] Saad Y and Schultz M H 1986 *SIAM J. Sci. Comput.* **7** (3) 856
[23] Fuloria D and Lee P D 2009 *Acta Mater.* **57** 5554